Sensor and Simulation Notes

Note 162

January 1973

The Reduction of Wasted Energy Delivered Outside of a Parallel-Plate Simulator Fed by a Sloped Source Array

by

M. I. Sancer and A. D. Varvatsis
Northrop Corporate Laboratories
Pasadena, California

Abstract

The time dependent surface current density that is induced on the outer surface of a planar source array of a parallel-plate simulator is calculated and an energy theorem is presented which relates this current to the energy delivered outside of the working volume of the simulator. Using the calculated current together with the energy theorem, it is shown that decreasing the slope of the source array or increasing the slope of the adjacent ground reduce the amount of wasted energy. For certain finite times of interest, this result is obtained by using numerical integration; however, in the infinite time limit analytic formulae are derived that clearly demonstrate the dependences of wasted energy on the slope angles of the source array and the adjacent ground.

I. Introduction

As a logical extension of a previous study concerning the effect of flanges on the sloped termination of a parallel-plate simulator [1], we consider the effect of flanges on the radiating properties of a sloped planar source array. We relate the angle of the flange to the sloping of the ground adjacent to the source array and then calculate the surface current density on the outside portion of the array. It is this current that delivers wasted energy outside of the working volume of the simulator.

In the calculation of this surface current density, we use the termination analysis. We show that it is possible to obtain an expression for this current by making suitable variable changes in the current formulae presented in the termination study. Even though these currents are simply related, we cannot make use of the numerical results for the termination current. After obtaining our expression for the source current, we require a separate numerical integration to obtain our results. These numerical results are presented as time dependent plots.

In a previous note [2], Baum used qualitative arguments to arrive at the conclusion that there was benefit to be gained by decreasing the slope angle of the source array, ξ, as well as benefit to increasing the slope of the ground adjacent to the source, δ (see figure 1). In order to quantitatively examine the effect of these two parameters, we derive an energy theorem that relates the current that we calculate to the wasted energy delivered outside of the working volume of the simulator. We show that the wasted energy is a triple integral that must be evaluated numerically when the source is turned on for a finite length of time. We present tables of the wasted energy for two finite times of interest and for various ξ's and δ's. For the infinite time limit, we analytically derive formulae for ratios of wasted energy that show the effect of varying ξ and δ. These formulae are algebraic functions of ξ and δ that can readily be examined. Both the numerical integration and our analytic expressions show that the wasted energy can be reduced by decreasing ξ and increasing δ.

II. Explicit Representation of the Induced Current

In a previous note on a termination problem for a parallel-plate simulator [1], we derived an expression for the magnetic field that is induced on the outer portion of the termination plane. In that note we mentioned that the source problem treated in this note could be related to the termination problem. The discussion relating these two analyses is facilitated by referring to figure 1. Repeating (21) of reference 1, we have

$$H_z(\rho) = \int_o^d d\rho_o G(\rho,\rho_o)\sin\xi\varepsilon_o F\left[\frac{\partial E_y}{\partial t}\right] \tag{1}$$

The quantity $H_z(\rho)$ is the magnetic field induced on the outer portion (region 1) of the source or termination plane. The quantities ρ, ρ_o, d, and ξ appear in figure 1 and are equally appropriate for either the source or termination problem. The source for the magnetic field is the Fourier transform of the time derivative of the y component of the electric field on either the source or termination plane ($F[\partial E_y/\partial t]$). The Green's function $G(\rho,\rho_o)$ is exactly the same for either problem and ε_o is the dielectric permittivity of free space. For the termination problem $H_z(\rho)$ was treated in detail when $E_y(t)$ was given by

$$E_y(t) = -E_o U(t - (v_o/c)\cos\xi) \tag{2}$$

where U is the Heavyside step function. In this note we would like to calculate $H_z(\rho)$ when $E_y(t)$ is given by

$$E_y(t) = -E_o U(t - (\rho_o/c)\cos\xi) \tag{3}$$

In (2), the termination problem, t = 0 corresponds to the incident wave striking the junction of the top plate and upper flange, while in (3), t = 0 corresponds to the source array being turned on at the junction of the bottom plate and lower flange. For out source problem we will label t as t_s to distinguish it from the t of the termination problem. Specifically we are interested in the inverse Fourier transform of $H_z(\rho)$, $F^{-1}H_z(\rho) = H_z(\rho,t_s)$, when it is given by

$$H_z(\rho) = \int_o^d d\rho_o G(\rho,\rho_o)\sin\xi\varepsilon_o F\left[\frac{\partial E_y}{\partial t_s}\right] \tag{4}$$

where

$$E_y(t_s) = -E_o U(t_s - (\rho_o/c)\cos\xi) \tag{5}$$

Using the relation

$$\rho_o = d - v_o \tag{6}$$

and defining the quantities t^* and γ as

$$\gamma = \pi - \xi \tag{7}$$

and

$$t^* = t_s + (d/c)\cos\gamma \tag{8}$$

we see that (4) and (5) become

$$H_z(\rho) = \int_o^d d\rho_o G(\rho,\rho_o)\sin\xi\,\varepsilon_o F\left[\frac{\partial E_y}{\partial t^*}\right] \tag{9}$$

and

$$E_y(t^*) = -E_o U(t^* - (v_o/c)\cos\gamma) \tag{10}$$

Comparing (9) and (10) with (1) and (2), we see that we can use the termination analysis evaluation of $H_z(\rho,t)$ provided we can separate the t and ξ dependence that are due to $G(\rho,\rho_o)$ from the t and ξ dependence due to $E_y(t)$. To do this we present $G(\rho,\rho_o)$ from reference 1. It is

$$G(\rho,\rho_o) = G_1(\rho,\rho_o) + G_2(\rho,\rho_o) \tag{11}$$

where

$$G_1(\rho,\rho_o) = -\frac{i}{2} H_o^{(1)}[k|\rho - \rho_o|] \tag{12a}$$

and

$$G_2(\rho,\rho_o) = \frac{iq\sin q\pi}{2\pi}\int_o^\infty dp\,\frac{H_o^{(1)}[k(\rho^2+\rho_o^2+2\rho\rho_o\cosh p)^{\frac{1}{2}}]}{\cosh qp - \cos q\pi} \tag{12b}$$

The only ω dependence that appears in $G(\rho,\rho_o)$ is in k which is the free space

wave number, ω/c, where c is the speed of light. The only ξ dependence contained in $G(\rho,\rho_o)$ appears in q which is given by

$$q = \pi/(\pi + \delta - \xi) \tag{13}$$

where δ is the slope angle of the adjacent ground (see figure 1). We are now in a position to describe the change of variables necessary to obtain $H_z(\rho,t_s)$ for the source problem from $H_z(\rho,t)$ for the termination problem. First we exhibit the functional dependence of $H_z(\rho,t)$ in more detail. It is

$$H_z(\rho,t) = H_z(\rho,t,\xi,q(\xi)) \tag{14}$$

We obtain $H_z(\rho,t_s)$ as

$$H_z(\rho,t_s) = H_z(\rho,t^*,\gamma,q(\xi)) \tag{15}$$

where t^* and γ are defined in (7) and (8). Defining

$$j = \frac{Z_o}{E_o} H_z(\rho,t_s) \tag{16}$$

and performing the substitution indicated in (15) in the $H_z(\rho,t,\xi,q(\xi))$ given in reference 1, we obtain

$$\begin{aligned} j = {} & U(\tau) - 1/\pi\, U(\tau - \tau_1)\arccos[\tau^{-1}(\alpha \sin \xi + \tau \cos \xi)] \\ & - 1/\pi\, U(\tau - \tau_2)\arccos[\tau^{-1}((1 - \alpha)\sin \xi - \tau \cos \xi)] \\ & - q/\pi^2 \sin q\pi\{[U(\tau - \tau_2) - U(\tau - \tau_3)]I_A + U(\tau - \tau_3)I_B\} \end{aligned} \tag{17}$$

where

$$\tau = \frac{ct_s - \rho \cos \xi}{d \sin \xi} = \frac{ct_s - \rho \cos \xi}{h} \tag{18}$$

$$\tau_1 = \alpha \frac{1+\cos \xi}{\sin \xi} \tag{19}$$

$$\tau_2 = (1 - \alpha)\,\frac{1-\cos\xi}{\sin\xi} \tag{20}$$

$$\alpha = v/d = 1 - \rho/d \tag{21}$$

$$\tau_3 = \tau_2 + \frac{1+\cos\xi}{\sin\xi} \tag{22}$$

$$I_A = \int_o^1 A(y)\arccos g(y)dy \tag{23}$$

$$I_B = I_{B_1} + I_{B_2} \tag{24}$$

$$I_{B_1} = \int_o^{y_I} A(y)\arccos g(y)dy \tag{25}$$

$$I_{B_2} = \int_{y_I}^1 A(y)\{\arcsin[g(y) + e(y)] - \arcsin g(y)\}dy \tag{26}$$

$$A(y) = 2y^{q-1}/(y^{2q} - 2y^q \cos q\pi + 1) \tag{27}$$

$$g(y) = C(C^2 + D^2)^{-\frac{1}{2}} \tag{28}$$

$$C = y^2 + 2y\beta \cos\xi + 1 \tag{29}$$

$$D^2 = 4y^2(\beta^2 - 1)\sin^2\xi \tag{30}$$

$$e(y) = 2y \sin^2\xi/[(1 - \alpha)(C^2 + D^2)^{\frac{1}{2}}] \tag{31}$$

$$\beta = \frac{\tau \sin \xi}{1-\alpha} + \cos \xi \tag{32}$$

$$y_I = 1 + \Gamma - ((1 + \Gamma)^2 - 1)^{\frac{1}{2}} \tag{33}$$

$$\Gamma = [(\beta(1 - \alpha) - \cos \xi)^2 - (2 - \alpha)^2]/[2(1 - \alpha)] \tag{34}$$

In comparing this j with the one contained in reference 1, it is important to observe that the same symbol, τ, is used to define different normalized times in each note. We did not add the appropriate subscript "s" to the τ defined in (18) in order to avoid this additional notation in the remaining part of the note.

The j as defined in (17) with appropriate auxiliary definitions is the form that was treated numerically in order to obtain the data for the plots of j versus τ that are presented in this note. In these plots the quantities ξ, δ, and α serve as parameters. For α not equal to 0 or 1, the value of j at $\tau = 0$ is unity for any ξ and δ. When $\alpha = 0$ we can immediately evaluate j at $\tau = 0$ to obtain

$$j(0) = 1 - \xi/\pi \qquad (\alpha = 0) \tag{35}$$

When $\alpha = 1$ we can use the results of reference 1 together with (15) to obtain an analytic expression for all τ. It is

$$j = q/\pi\{\xi U(\tau) - U(\tau - \tau_1)\arccos[\tau^{-1}(\sin \xi + \tau \cos \xi)]\} \tag{36}$$

where τ_1 is given in (19) with $\alpha = 1$. From (36) we see that

$$j(0) = (\xi/\pi)q = \xi/\pi(1 + \delta/\pi - \xi/\pi)^{-1} \qquad (\alpha = 1) \tag{37}$$

Finally, to take full advantage of the termination results we apply (15) to the case $\xi = \pi/2$ and $\delta = 0$. For this case

$$j = U(\tau) - 1/\pi\ U(\tau - \alpha)\arccos(\alpha/\tau) - 1/\pi\ U(\tau - (2 - \alpha))\arccos((2 - \alpha)/\tau) \quad (38)$$

Equation (38) will be particularly useful for our subsequent energy analysis.

III. Energy Theorem

Due to the symmetry of the boundaries of the simulator and excitation we know that the electric field has no z component, while the magnetic field has only a z component (see figure 1). We now write Maxwell's equations as

$$\nabla\times\underline{E} = -\mu_o\hat{a}_z \frac{\partial H_z}{\partial t_s} \tag{39}$$

$$\nabla\times\hat{a}_z H_z = \varepsilon_o \frac{\partial \underline{E}}{\partial t_s} \tag{40}$$

where ∇ operates only on the coordinates transverse to z. The t_s that appears in (39) and (40) is measured from the time that the lowest element in the source array is fired and to be consistent , the subscript "s" is used. Taking the scalar product of both sides of (39) with $\hat{a}_z H_z$ and of (40) with $\underline{E}$, then subtracting and using a standard identity, we obtain

$$\nabla\cdot[\underline{E}\times\hat{a}_z H_z] = -\frac{\mu_o}{2}\frac{\partial|H_z|^2}{\partial t_s} - \frac{\varepsilon_o}{2}\frac{\partial|\underline{E}|^2}{\partial t_s} \tag{41}$$

We now integrate (41) over region 1 (see figure 1) and use the divergence theorem to obtain

$$-\int_o^d d\rho\hat{n}\cdot[\underline{E}\times\hat{a}_z H_z] = \int d\ell\hat{n}\cdot[\underline{E}\times\hat{a}_z H_z] + \int_A\left(\frac{\mu_o}{2}\frac{\partial|H_z|^2}{\partial t_s} + \frac{\varepsilon_o}{2}\frac{\partial|\underline{E}|^2}{\partial t_s}\right)dA \tag{42}$$

The first integral on the right hand side of (42) is over the dashed contour bounding region 1 and the second is over region 1. The integral on the left hand side can be written as

$$-\int_o^d d\rho n\cdot[\underline{E}\times\hat{a}_z H_z] = -\int_o^d d\rho \sin\xi E_y H_z \tag{43}$$

The H_z that appears in (43) is the one calculated in the previous section and E_y is the source field given in (5). Let us now consider that E_y is given by the following expression rather than (5). It is

$$E_y(t_s) = -E_o[U(t_s - (\rho_o/c)\cos\xi) - U(t_s - t_m - (\rho_o/c)\cos\xi] \tag{44}$$

This expression corresponds to each element of the source array being sequentially turned off after a time t_m has elapsed since it was sequentially turned on. The reason it is now desirable to consider $E_y(t_s)$ to be given by (44) rather than (5) is to avoid infinite energies. It is also physically meaningful to consider the case where the elements of the source array are only turned on for a finite length of time since the EMP that is simulated only lasts for a finite time. Eventually we will allow t_m to approach infinity and still obtain a meaningful answer by considering a ratio fo energies which causes the infinities to cancel. Using (16), (18) and (44) in the integral contained in the right hand side of (43) we obtain

$$- \sin \xi \int_o^d d\rho E_y H_z = \frac{E_o^2}{Z_o} \sin \xi \int_o^d d\rho [U(\tau) - U(\tau - T)] j(\alpha,\tau) \tag{45}$$

where

$$T = \frac{ct_m}{h} \tag{46}$$

We note that $j(\alpha,\tau)$ for the excitation described in (44) is the same $j(\alpha,\tau)$ for the excitation described in (5) for $\tau < T$. Using (21) to change the ρ variable of integration to α, the integral in (45) becomes

$$\int_o^d d\rho [U(\tau) - U(\tau - T)] j(\alpha,\tau) = d \int_o^1 d\alpha [U(\tau) - U(\tau - T)] j(\alpha,\tau) \tag{47}$$

We can now write (42) as

$$\frac{E_o^2}{Z_o} h \int_o^1 d\alpha [U(\tau) - U(\tau - T)] j(\alpha,\tau) = \int d\ell \hat{n} \cdot [\underline{E} \times \hat{a}_z H_z]$$

$$+ \int_A \left(\frac{\mu_o}{2} \frac{\partial |H_z|^2}{\partial t_s} + \frac{\varepsilon_o}{2} \frac{\partial |\underline{E}|^2}{\partial t_s} \right) dA \tag{48}$$

where we have used the relation $h = d \sin \xi$. Equation (48) is a relationship involving power. We now integrate both sides of this equation with respect to t_s from 0 to t_m to obtain our energy relationship. It is

$$E(\xi,\delta,T) = \int_o^{t_m} dt_s \int d\ell \hat{n} \cdot [\underline{E} \times \hat{a}_z H_z] + \int_o^{t_m} dt_s \int_A \left(\frac{\mu_o}{2} \frac{\partial |H_z|^2}{\partial t_s} + \frac{\varepsilon_o}{2} \frac{\partial |\underline{E}|^2}{\partial t_s} \right) dA \tag{49}$$

where

$$E(\xi,\delta,T) = \frac{E_o^2}{Z_o} h \int_o^{t_m} dt_s \int_o^1 d\alpha [U(\tau) - U(\tau - T)] j(\alpha,\tau) \tag{50}$$

The first term on the right hand side of (49) corresponds to the energy wasted through radiation and the second term corresponds to the wasted energy stored in region 1. The source for both forms of wasted energy is $E(\xi,\delta,T)$. Combining (18) and (21) we obtain a form for a change of variables that will simplify the evaluation of (50). That is

$$t_s = \frac{h}{c}\tau + \frac{(1-\alpha)}{c}\cos\xi \tag{51}$$

enables $E(\xi,\delta,T)$ to be written as

$$E(\xi,\delta,T) = \frac{E_o^2}{Z_o}\frac{h^2}{c} I(\xi,\delta,T) \tag{52}$$

where

$$I(\xi,\delta,T) = \int_o^1 d\alpha \int_o^T d\tau j(\alpha,\tau) \tag{53}$$

with T given by (46) and the previous section was devoted to defining $j(\alpha,\tau)$. For general ξ, δ, and T, $I(\xi,\delta,T)$ must be evaluated numerically. This is complicated by the fact that the determination of j, in general, requires a single numerical integration so that the evaluation of I requires a triple numerical integration. In order to test the numerical integration we will evaluate I analytically for special cases. Finally we will obtain the long time asymptotic behavior of I for arbitrary ξ and δ. The remaining analysis to be presented in this note will be devoted to analytically treating I.

IV. Analytic Evaluation of Energy for $\xi = \pi/2$ and $\delta = \pi/2$

In order to obtain the analytic representation for this case, we set $\xi = \delta = \pi/2$ in (17) and the corresponding defining equations. The resulting expression is

$$j = U(\tau) - 1/\pi\ U(\tau - \alpha)\arccos(\alpha/\tau) - 1/\pi\ U(\tau - (1 - \alpha))\arccos((1 - \alpha)/\tau) \quad (54)$$

Substituting (54) into (53), the resulting expression to be evaluated is

$$I = I_1 + I_2 \quad (55)$$

where

$$I_1 = \tfrac{1}{2} \int_0^1 d\alpha \int_0^\alpha d\tau + 1/\pi \int_0^1 d\alpha \int_\alpha^T d\tau(\pi/2 - \arccos(\alpha.\tau)) \quad (56)$$

and

$$I_2 = \tfrac{1}{2} \int_0^1 d\alpha \int_0^{1-\alpha} d\tau + 1/\pi \int_0^1 d\alpha \int_{1-\alpha}^T d\tau(\pi/2 - \arccos((1 - \alpha)/\tau)) \quad (57)$$

We now make the change of variables in (57), $\alpha' = 1 - \alpha$, to show that

$$I_1 = I_2 \quad (58)$$

so that

$$I = 2I_1 \quad (59)$$

We now rewrite I_1 by evaluating the first integral on the right hand side of (56) and using the identity

$$\arcsin x = \pi/2 - \arccos x \quad (60)$$

in the second to obtain

$$I_1 = 1/4 + 1/\pi\ I_3 \quad (61)$$

where

$$I_3 = \int_0^1 d\alpha \int_\alpha^T d\tau \arcsin(\alpha/\tau) \tag{62}$$

An evaluation of the τ integration can be found in the book by Gradshteyn and Ryzhik [3]. Performing the τ integration, and subsequent α integration where is is trivial, we can write I_3 as

$$I_3 = -\pi/4 + T \int_0^1 d\alpha \arcsin(\alpha/T) - \int_0^1 d\alpha\alpha \ln \alpha + \int_0^1 d\alpha\alpha \ln[T + (T^2 - \alpha^2)^{\frac{1}{2}}] \tag{63}$$

The first two integrals in the right hand side of (63) can be found in many different tables of integrals or can be evaluated by integrating by parts. The resulting expressions are

$$\int_0^1 d\alpha \arcsin \alpha/T = \arcsin(1/T) - T(1 - A) \tag{64a}$$

where

$$A = (1 - T^{-2})^{\frac{1}{2}} \tag{64b}$$

and

$$\int_0^1 d\alpha\alpha \ln \alpha = -1/4 \tag{65}$$

The remaining integral is put into a more recognizable form by making the change of variables

$$y = (T^2 - \alpha^2)^{\frac{1}{2}} \tag{66}$$

The resulting integral can then be expressed as

$$\int_0^1 d\alpha\alpha \ln[T + (T^2 - \alpha^2)^{\frac{1}{2}}] = \int_{AT}^T dyy \ln(T + y) \tag{67}$$

The right hand side of (67) is now in a form where it is readily found in many tables of integrals or it can be evaluated by integrating by parts.

$$\int_{AT}^T dyy \ln(T + y) = -1/4 + 1/2[T^2(1 - A) + \ln[T(1 + A)]] \tag{68}$$

Combining our results we have

$$I = 2T \arcsin(1/T) - T^2(1 - A) + \ln[T(1 + A)] \tag{69}$$

This expression is useful as a check on the numerical integration of I for general ξ and δ. In particular the evaluation of I for $\xi = \pi/2$ and $\delta = 0$ was performed in several ways as part of our debugging procedure. This case will be treated in the next section.

V. Analytic Evaluation of Energy for $\xi = \pi/2$ and $\delta = 0$

The evaluation of $I(\pi/2,0,T)$ was obtained using two different approaches. It was obtained by using the program for general ξ, δ, and T and then choosing $\delta = 10^{-3}\pi$. This served as a check on the program because we can obtain an analytic evaluation of this quantity. The explicit representation of I is found by substituting (38) into (53) to obtain

$$I(\pi/2,0,T) = I_o = \int_o^1 d\alpha \int_o^T d\tau[U(\tau) - 1/\pi\ U(\tau - \alpha)\arccos \alpha/\tau$$

$$-1/\pi\ U(\tau - (2 - \alpha))\arccos((2 - \alpha)/\tau)] \tag{70}$$

Using the change of variables

$$\tau_o = \tau/2 \tag{71}$$

and

$$\alpha_o = \alpha/2 \tag{72}$$

we can rewrite (70) as

$$I_o = 4 \int_o^{\frac{1}{2}} d\alpha_o \int_o^{T/2} d\tau_o[U(\tau_o) - 1/\pi\ U(\tau_o - \alpha_o)\arccos \alpha_o/\tau_o$$

$$-1/\pi\ U(\tau_o - (1 - \alpha_o))\arccos((1 - \alpha_o)/\tau_o)] \tag{73}$$

Because the integral in (73) is symmetric about $\alpha_o = \frac{1}{2}$, it can be written as

$$I_o = 2 \int_o^1 d\alpha_o \int_o^{T/2} d\tau_o[U(\tau_o) - 1/\pi\ U(\tau_o - \alpha_o)\arccos \alpha_o/\tau_o$$

$$-1/\pi\ U(\tau_o - (1 - \alpha_o))\arccos((1 - \alpha_o)/\tau_o)] \tag{74}$$

Comparing (74) with (55) and its corresponding defining equations, we see that

$$I(\pi/2,0,T) = 2I(\pi/2,\pi/2,T/2) \tag{75}$$

Using the explicit representation of $I(\pi/2,\pi/2,T)$ given in (69), we have

$$I(\pi/2,0,T) = 2T \arcsin(2/T) - (T^2/2)(1 - A_o) + 2 \ln[(T/2)(1 + A_o)] \tag{76}$$

where

$$A_o = (1 - 4/T^2)^{\frac{1}{2}} \tag{77}$$

VI. Analytic Long Time Energy Relationship

In this section we will obtain the long time asymptotic behavior of I given by (53) with j given by (17) which is valid for arbitrary ξ and δ. We now express I as

$$I = I^{(1)} + I^{(2)} \tag{78}$$

where

$$I^{(1)} = \int_0^T d\tau \int_0^1 d\alpha \Big[U(\tau) - 1/\pi\, U(\tau - \tau_1)\arccos[\tau^{-1}(\alpha \sin \xi + \tau \cos \xi)]$$

$$- 1/\pi\, U(\tau - \tau_2)\arccos[\tau^{-1}((1 - \alpha)\sin \xi - \tau \cos \xi)]\Big] \tag{79}$$

$$I^{(2)} = \int_0^T d\tau \int_0^1 d\alpha(-q/\pi^2)\sin q\pi\{[U(\tau - \tau_2) - U(\tau - \tau_3)]I_A + U(\tau - \tau_3)I_B\} \tag{80}$$

The quantities τ_1, τ_2, τ_3, q, I_A, and I_B have been defined in section II. Because $I^{(1)}$ is a monotonically increasing function of T, the lower limit is unimportant in obtaining its asymptotic behavior. We now evaluate this quantity as

$$I^{(1)} \sim I_L^{(1)} \tag{81}$$

where

$$I_L^{(1)} = \int_{T_L}^T d\tau \int_0^1 d\alpha \Big[1 - 1/\pi \arccos[\tau^{-1}(\alpha \sin \xi + \tau \cos \xi)]$$

$$- 1/\pi \arccos[\tau^{-1}((1 - \alpha)\sin \xi - \tau \cos \xi)]\Big] \tag{82}$$

and T_L is chosen so that $T_L \geq T_1$ and $T_L \geq T_2$ for any α, i.e., $T_L = (1 + \cos \xi)/\sin \xi$. Our final expression will be independent of T_L. Using (60), we can rewirte (82) as

$$I_L^{(1)} = 1/\pi \int_{T_L}^{T} d\tau \int_o^1 d\alpha \Big[\arcsin[\tau^{-1}(\alpha \sin \xi + \tau \cos \xi)]$$

$$+ \arcsin[\tau^{-1}((1 - \alpha)\sin \xi - \tau \cos \xi)]\Big] \tag{83}$$

For large τ, the integrand in (83) behaves like

$$\arcsin[\tau^{-1}(\alpha \sin \xi + \cos \xi)] + \arcsin[\tau^{-1}((1 - \alpha)\sin \xi - \cos \xi)]$$

$$\sim \arcsin(\cos \xi) + \arcsin(-\cos \xi) + \frac{\alpha}{\tau} + \frac{1-\alpha}{\tau} = \frac{1}{\tau} \tag{84}$$

Substituting (84) into (83), adding the requirement $T >> T_L$, and performing the integrations, we obtain after combining the resulting integral with (81)

$$I^{(1)} \sim 1/\pi \ln T \qquad (T \to \infty) \tag{85}$$

We now consider the long time behavior of I_2. First we note

$$I^{(2)} \sim I_L^{(2)} \tag{86}$$

where

$$I_L^{(2)} = (-q/\pi^2)\sin q\pi \int_{T_L}^{T} d\tau \int_o^1 d\alpha I_B \tag{87}$$

We choose T_L so that it is larger than τ_3 for any α, i.e., $T_L = 2/\sin \xi$. We now refer back to (24) through (32) to determine the large τ behavior of I_B. Examining these equations, we see that

$$I_B \sim \tau^{-1} \int_o^1 A(y)dy \tag{88}$$

with $A(y)$ given in (27). Making the change of variables

$$y = e^{-p} \tag{89}$$

we have

$$\int_0^1 A(y)dy = \int_0^\infty dp(\cosh qp - \cos q\pi)^{-1} \tag{90}$$

The right hand side of (90) was evaluated in reference 1, and is given by

$$\int_0^\infty dp(\cosh qp - \cos q\pi)^{-1} = \frac{\pi}{q}(1 - q)/\sin q\pi \tag{91}$$

Combining (88), (90), (91), substituting the result into (87), and performing the remaining integrations we obtain for $T \gg T_L$

$$I_L^{(2)} \sim -(1 - q)/\pi \ln T \qquad (T \to \infty) \tag{92}$$

Our resulting asymptotic expression for I is obtained by combining (78), (85), (86) and (92). The final expression is

$$I(\xi,\delta,T) \sim q/\pi \ln T \qquad (T \to \infty) \tag{93}$$

where q is given in (13). Our final results are obtained by forming physically meaningful ratios. Using the relationship between the wasted energy $E(\xi,\delta,T)$ and $I(\xi,\delta,T)$ given in (52) as well as the explicit representation of q given in (13), we obtain

$$E(\xi,\delta,\infty)/E(\xi,0,\infty) = (1 + \delta/(\pi - \xi))^{-1} \tag{94}$$

This expression shows how the wasted energy is decreased by increasing the slope of the ground adjacent to the source array (see figure 1). It is also meaningful to form the following ratio of energies again using (93), (52), and (13)

$$E(\xi,\delta,\infty)/E(\pi/2,\delta,\infty) = \frac{1-(\frac{1}{2})(1+\delta/\pi)^{-1}}{1-(\xi/\pi)(1+\delta/\pi)^{-1}} \tag{95}$$

This expression shows how the wasted energy is decreased by decreasing the slope angle of the source array.

VII. Results

Because we related this source analysis to our previous termination analysis [1], it was convenient to calculate our induced surface current density for the same values of the geometrical parameters (ξ,δ,α) that were used for the termination problem. Out data is presented in the following manner. For each orientation described by a particular ξ and δ, we present plots of the induced current after it has been normalized versus the appropriately normalized time, τ, at the center of the source array (α = .5). The normalizing relations are given in (16) and (18). These plots are presented in figures 2 through 5. In figure 6 we also show how the current varies over the array for $\xi = \pi/4$ and $\delta = 0$. We augment this sample of waveforms by presenting the following tables.

Table 1.

τ_w's for $\xi = \pi/2$

α \ δ	0	$\pi/12$	$\pi/6$	$\pi/4$	$\pi/3$	π
0	6.47	5.58	4.91	4.39	3.94	2.09
.1	6.46	5.56	4.90	4.36	3.92	2.07
.5	6.41	5.51	4.84	4.31	3.87	2.06
.9	6.39	5.49	4.81	4.28	3.86	2.14
1.0	6.39	5.49	4.81	4.28	3.86	2.20

Table 2.

τ_w's for $\xi = \pi/3$

α \ δ	0	$\pi/12$	$\pi/6$	$\pi/4$	$\pi/3$	π
0	4.68	4.15	3.70	3.31	2.97	1.94
.1	4.72	4.18	3.73	3.34	3.01	1.94
.5	4.87	4.34	3.90	3.53	3.21	1.95
.9	5.06	4.54	4.12	3.77	3.48	2.23
1.0	5.12	4.60	4.18	3.84	3.56	2.38

Table 3.

τ_w's for $\xi = \pi/4$

α \ δ	0	$\pi/12$	$\pi/6$	$\pi/4$	$\pi/3$	π
0	4.05	3.58	3.16	2.79	2.54	1.96
.1	4.11	3.64	3.23	2.87	2.60	1.99
.5	4.40	3.96	3.57	3.24	2.95	2.18
.9	4.76	4.34	4.00	3.71	3.46	2.46
1.0	4.86	4.45	4.12	3.85	3.62	2.68

Table 4.

τ_w's for $\xi = \pi/10$

α \ δ	0	$\pi/12$	$\pi/6$	$\pi/4$	$\pi/3$	π
0	2.30	2.19	2.12	2.06	2.02	1.88
.1	2.52	2.41	2.33	2.27	2.22	2.06
.5	3.84	3.69	3.58	3.51	3.46	3.30
.9	5.82	5.72	5.52	3.10	2.28	1.18
1.0	6.34	6.30	*	*	*	*

*The value of j at $\tau = 0$ is given in (37) as $j(0) = .1/(.9 + \delta/\pi)$ and is below .1 for these special cases.

Table 5.

τ_I's

α \ ξ	$\pi/2$	$\pi/3$	$\pi/4$	$\pi/10$
* 0	1.00	.58	.41	.16
.1	.10	.17	.24	.14
.5	.50	.29	.21	.08
.9	.90	.58	.04	.02
† 1.0	1.00	1.73	2.41	6.31

*The initial value for $\alpha = 0$ is given in (35) as $j(0) = 1 - \xi/\pi$.
†The initial value for $\alpha = 1$ is given in (37) as $j(0) = \xi/\pi\ (1 + \delta/\pi - \xi/\pi)^{-1}$.

Tables 1 through 4 contain the pulse width, τ_w, of the induced surface current density. This is the length of time, measured in units of h/c, for the normalized current to decrease to .1. Table 5 contains the normalized time, τ_I, that this current stays at its peak value. Again, τ_I is time measured in units of h/c. For the step function excitation we are considering, it is known that there is zero rise time to this peak value, and the numerical value of this peak (plateau) is either a unity or can be readily determined from the simple algebraic formulae given below the table.

Although the current waveforms are of interest, our results for the wasted energy corresponding to this current can be more readily used to assess the value of sloping the ground adjacent to the source array. In (52) we showed that the wasted energy for a particulat (ξ,δ) when the source was turned on for time, T, is given by

$$E(\xi,\delta,T) = \frac{E_o^2}{Z_o}\frac{h^2}{c} I(\xi,\delta,T)$$

Our energy results are presented in the following tables.

Table 6.

Values of $I(\xi,\delta)$ for T = 5

ξ \ δ	0	$\pi/12$	$\pi/6$	$\pi/4$	$\pi/3$	π
$\pi/2$	1.98	1.75	1.58	1.45	1.35	1.01
$\pi/3$	1.50	1.38	1.29	1.22	1.16	.94
$\pi/4$	1.30	1.22	1.15	1.10	1.06	.90
$\pi/10$	.84	.82	.80	.78	.77	.72

Table 7.

Values of $I(\xi,\delta)$ for $T = 10$

ξ \ δ	0	$\pi/12$	$\pi/6$	$\pi/4$	$\pi/3$	π
$\pi/2$	2.42	2.13	1.91	1.75	1.62	1.15
$\pi/3$	1.84	1.68	1.56	1.46	1.38	1.07
$\pi/4$	1.60	1.49	1.40	1.32	1.26	1.02
$\pi/10$	1.11	1.06	1.02	.99	.96	.85

The values of T used in these tables correspond to the elements in the array being turned on for a duration of 5h/c and 10h/c seconds. To augment these tables we repeat (94) and (95)

$$E(\xi,\delta,\infty)/E(\pi/2,\delta,\infty) = \frac{1-(\frac{1}{2})(1+\delta/\pi)^{-1}}{1-(\xi/\pi)(1+\delta/\pi)^{-1}}$$

$$E(\xi,\delta,\infty)/E(\xi,0,\infty) = (1 + \delta/(\pi - \xi))^{-1}$$

These relations together with tables 6 and 7 quantitatively show the benefit of decreasing ξ as well as increasing δ.

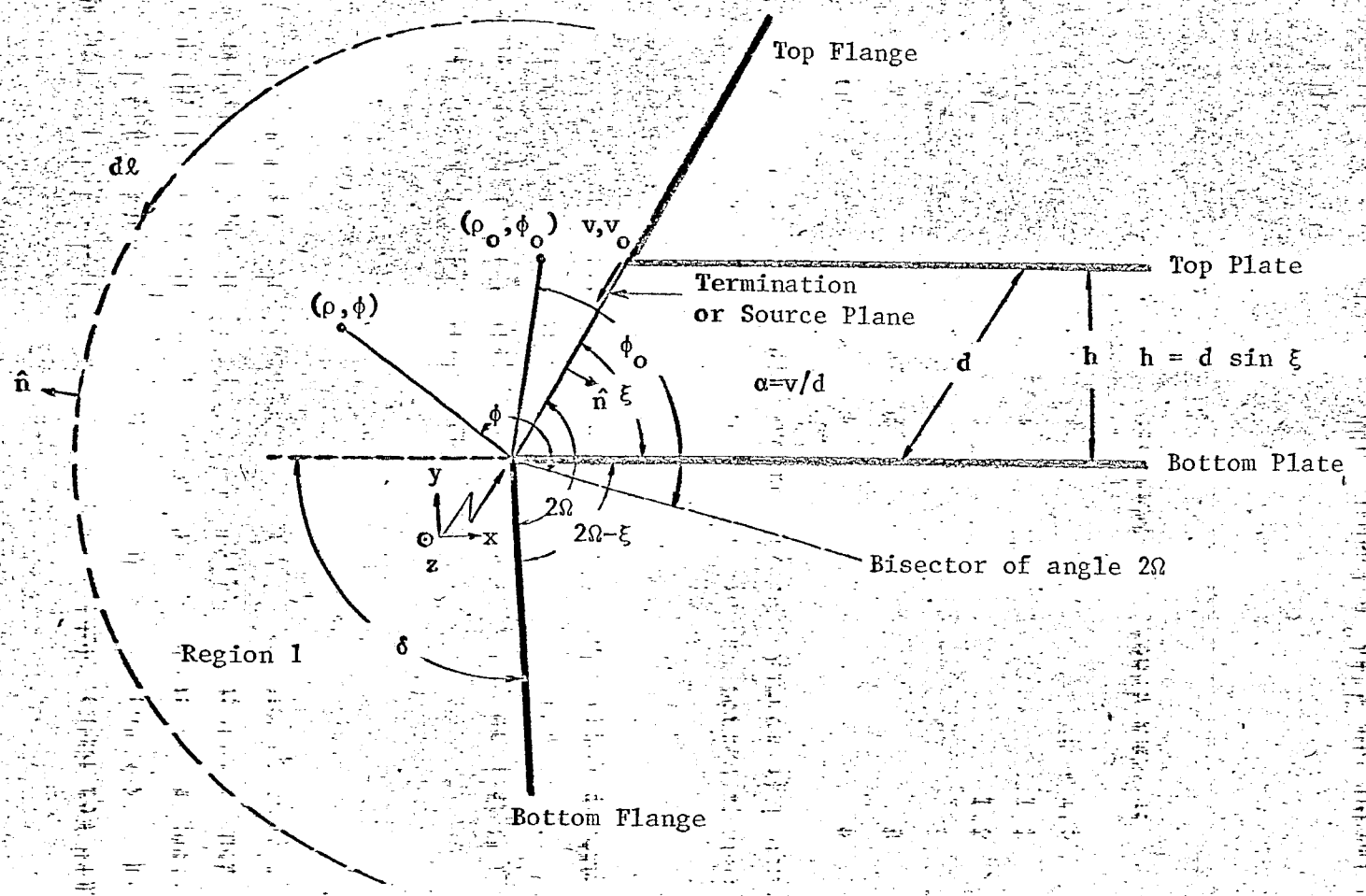

Figure 1. Geometry appropriate to varying the angle of the bottom flange.

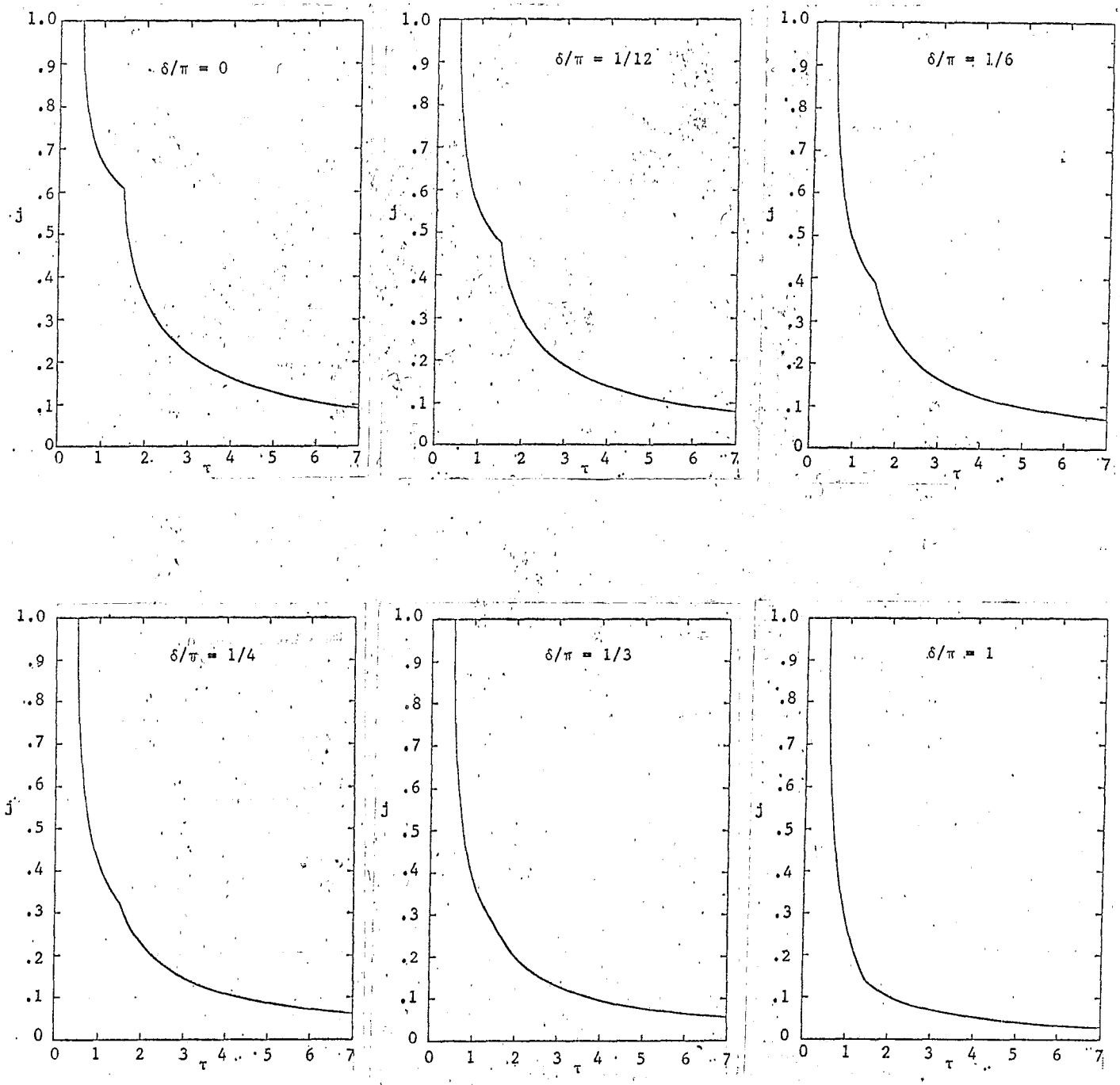

Figure 2. Induced surface current density, j, versus normalized time, τ, at the center of the source array, α = .5, for ξ = π/2 and six values of δ.

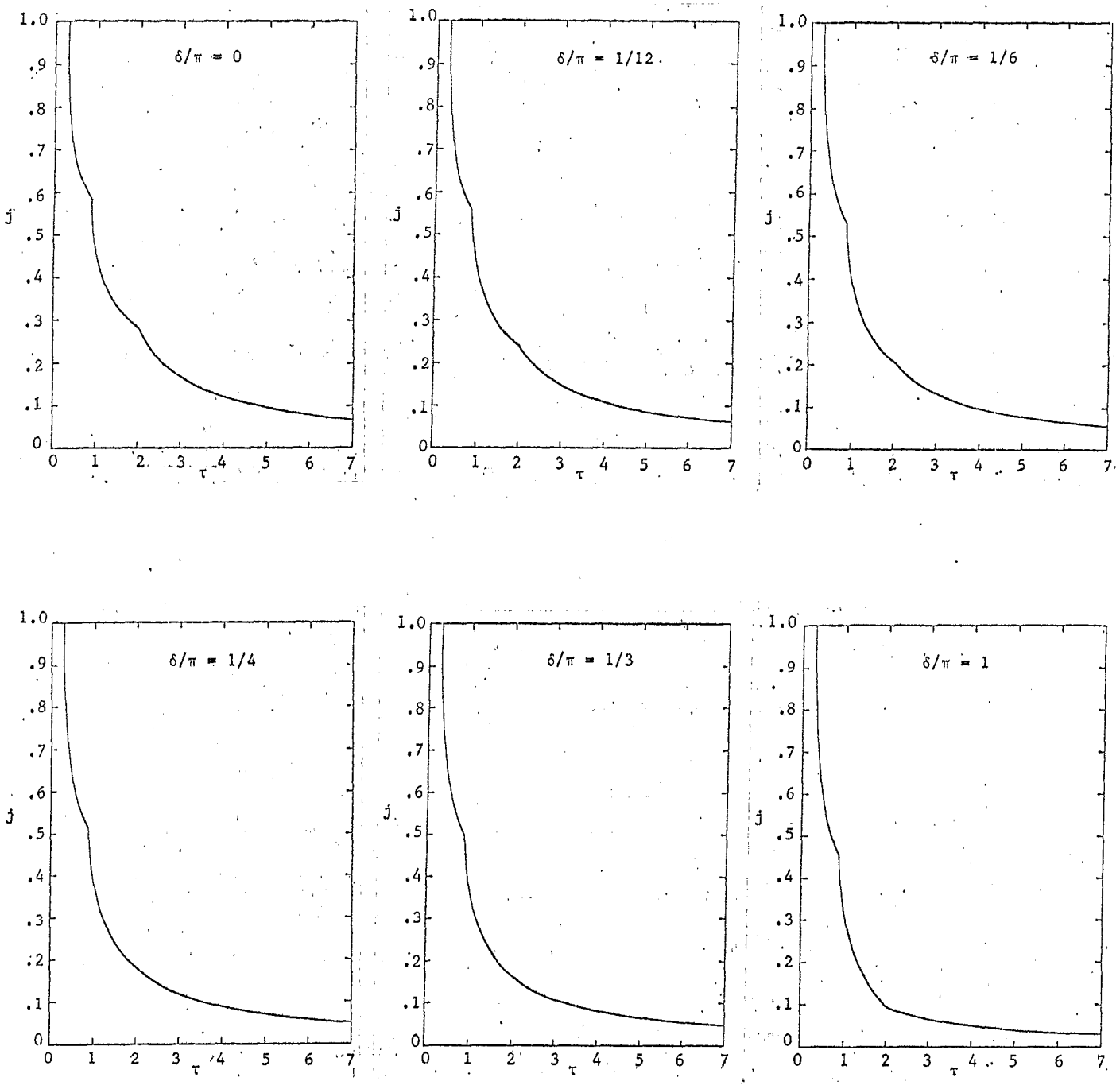

Figure 3. Induced surface current density, j, versus normalized time, τ, at the center of the source array, α = .5, for ξ = π/3 and six values of δ.

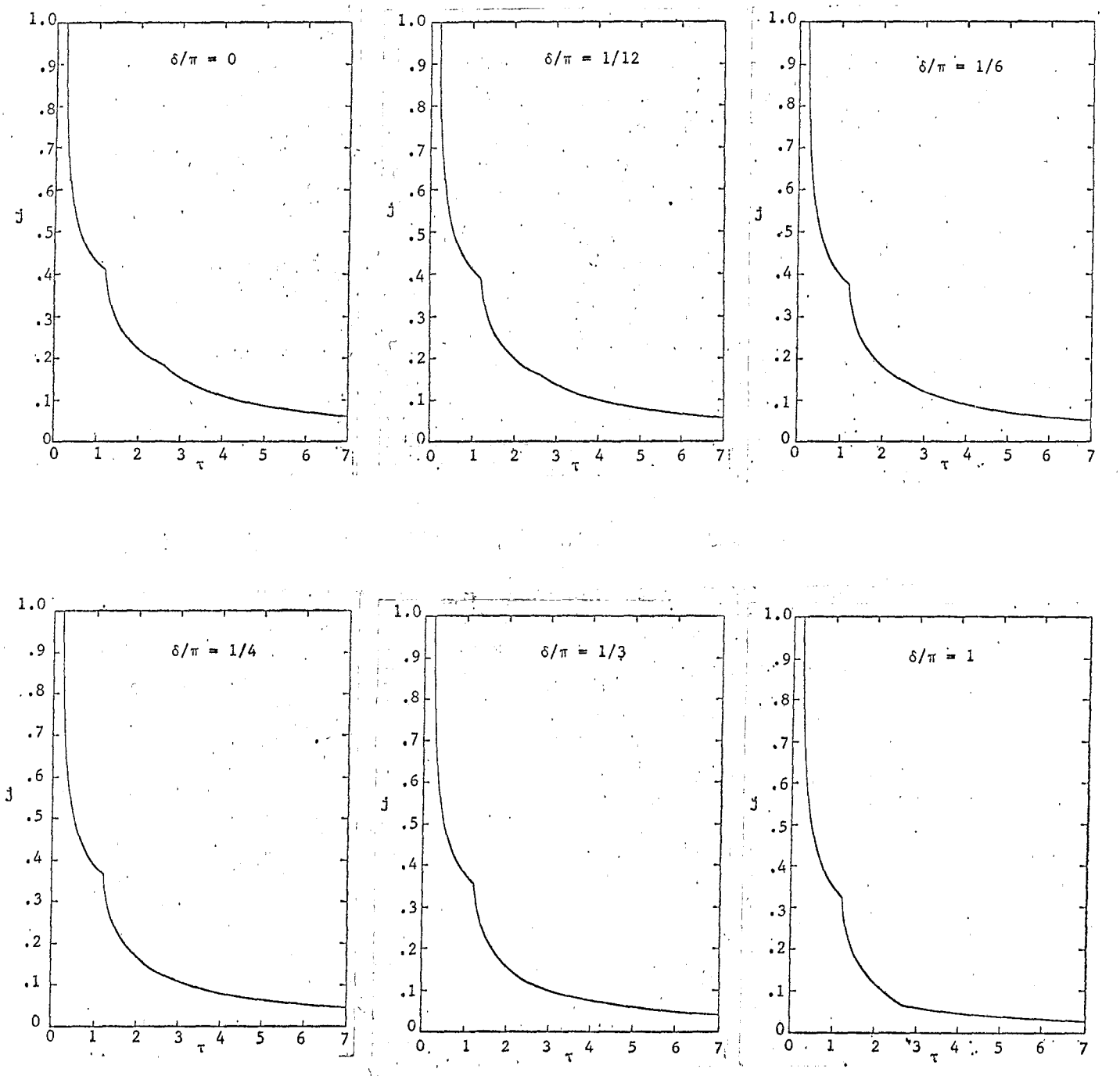

Figure 4. Induced surface current density, j, versus normalized time, τ, at the center of the source array, α = .5, for ξ = π/4 ans six values of δ.

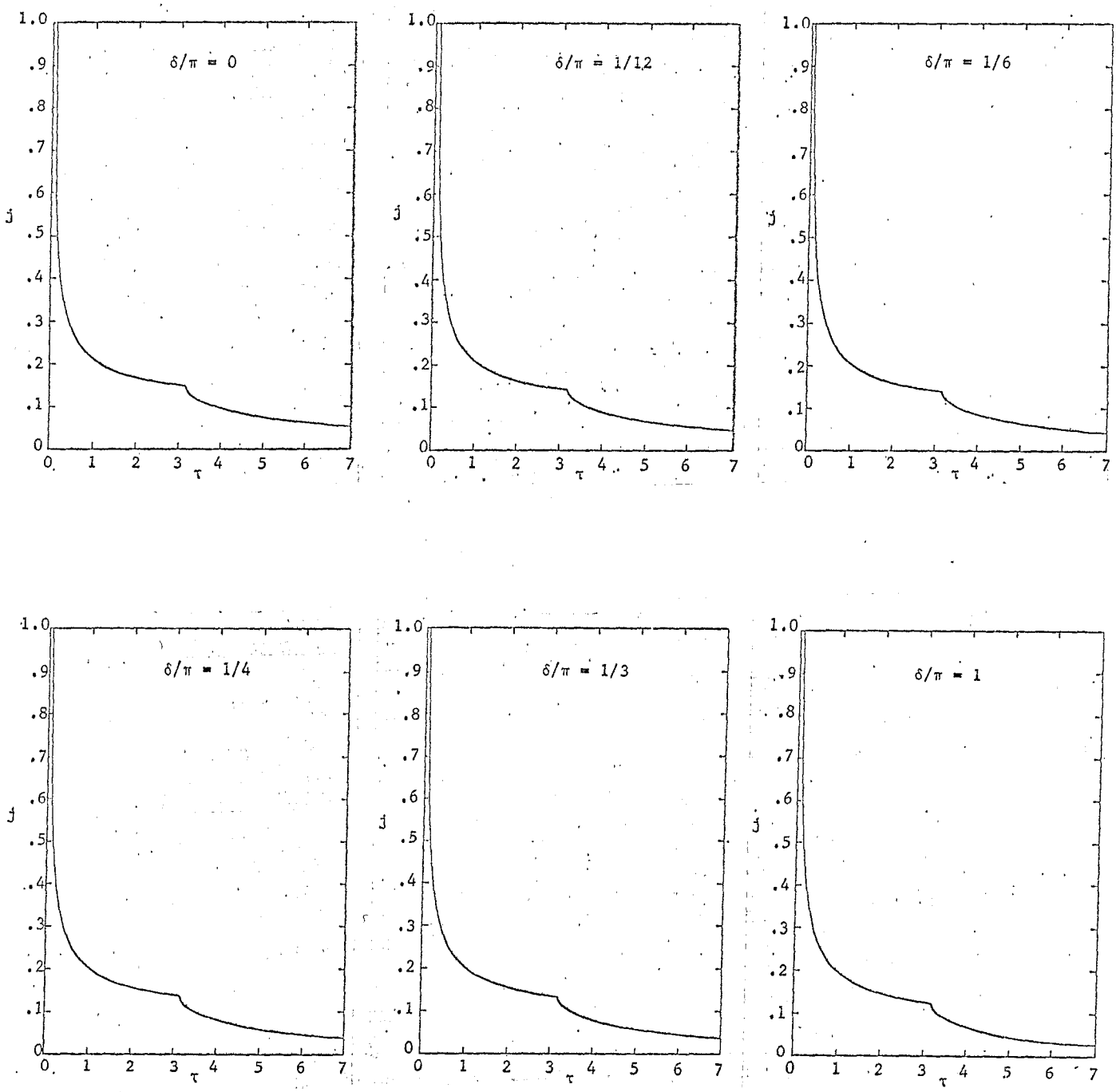

Figure 5. Induced surface current density, j, versus normalized time, τ, at the center of the source array, α = .5, for ξ = π/10 and six values of δ.

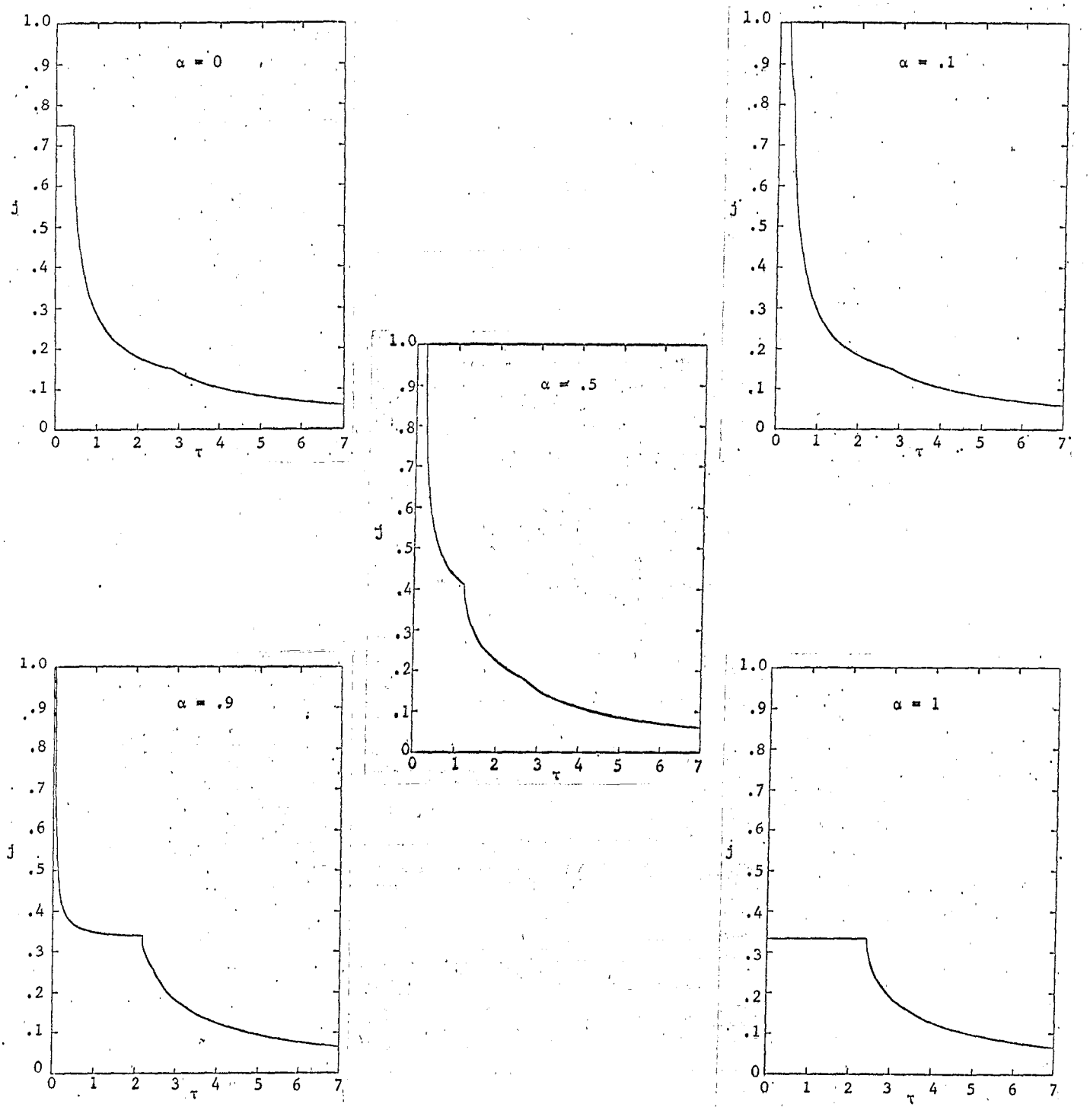

Figure 6. Induced surface current density, j, versus normalized time, τ, at 5 points on the source array for $\xi = \pi/4$ and $\delta = 0$.

Acknowledgement

We thank Dr. C. E. Baum for suggesting this study, Mr. R. W. Sassman for computer programming, and Mrs. G. Peralta for preparing this manuscript.

References

1. M. I. Sancer and A. D. Varvatsis, "The effect of flanges on the inductance of a sloped termination for a parallel-plate simulator," Sensor and Simulation Notes, Note , November 1972.
2. C. E. Baum, "General principles for the design of Atlas I and II, Part IV: additional considerations for the design of pulsar arrays," Sensor and Simulation Notes, Note 146, March 1972.
3. I. S. Gradshteyn and I. M. Ryzhik, Tables of Integrals, Series, and Products, Academic Press, New York, p. 207, 1965.